

Experimental study of high density plasma operation in Heliotron J

S. Kobayashi¹, T. Mizuuchi¹, Y. Nakashima², K. Nagasaki¹, H. Okada¹, T. Minami¹, S. Kado¹, S. Yamamoto¹, S. Ohshima¹, H. Y. Lee³, L. Zang³, Y. Nagae³, H. Fukushima³, K. Watanabe⁴, R. Seki⁴, K. Tanaka⁴, S. Murakami⁵, Y. Suzuki⁴, K. Mukai⁴, Y. Nakamura³, S. Konoshima¹, K. Yaguchi¹, T. Senju¹, M. Shibano¹, K. Toushi¹, K. Sakamoto¹, F. Sano¹

¹ Institute of Advanced Energy, Kyoto Univ., Uji, Kyoto 611-0011, JAPAN

² Plasma Research Center, Univ. of Tsukuba, Tsukuba, Ibaraki 305-8577, JAPAN

³ Graduate School of Energy Science, Kyoto Univ., Uji, Kyoto 611-0011, JAPAN

⁴ National Institute for Fusion Science, Toki, Gifu 509-5292, JAPAN

⁵ Graduate School of Engineering, Kyoto Univ., Kyoto 606-8501, JAPAN

1. Introduction

In magnetically confined plasmas, optimization of particle fuelling is an important subject to achieve high performance plasmas. In Heliotron J, several fuelling methods have been tried to control the plasma profile and to improve the performance: Supersonic molecular beam injection (SMBI) and shot-pulsed high-intensity gas puffing (HIGP). These methods have been applied aiming at core fuelling and reducing edge neutrals. For the optimization of the fuelling, it is important not only to reveal the confinement characteristics but also to investigate the behaviour of the neutrals in the peripheral region. Recently, we have obtained a high density plasma condition more than $1 \times 10^{20} \text{ m}^{-3}$ by the HIGP method [1, 2]. In this paper, we present the experimental result of the high density plasma operation by HIGP. The confinement characteristics and the behaviour of the hydrogen recycling in the high density plasma experiments are described.

2. Experimental results

Heliotron J is a medium-sized ($\langle R_0 \rangle / \langle a_p \rangle = 1.2 \text{ m} / 0.17 \text{ m}$) helical-axis heliotron device with an $L/M = 1/4$ helical coil, where L and M are the pole number of the helical coil and helical pitch number, respectively. The working gas was deuterium in this study. Two tangential beamlines of NBI have been installed in Heliotron J (BL1 and BL2). Each beamline has two bucket-type ion sources (hydrogen) and the maximum beam power and acceleration voltage of 0.7 MW and 30 keV, respectively. The mean pitch angle of the beam ions is about 155 (25) degree in the co- (counter-) injection case of the standard configuration of Heliotron J.

Figure 1 shows the waveform of a high density plasma discharge using the HIGP method, which was obtained in the NBI heated plasmas in the configuration with lower toroidal magnetic ripple component (low ε_t). A non-resonant (2.45GHz) microwave was launched before NB injection to initiate the seed plasma [3]. The co and counter NBs were

injected at the port through power of 0.4 and 0.7MW, respectively. An high-intensity gas fuelling, several times higher than that for the normal one with short period (10-20ms), was applied from $t=210$ ms. In this period, small degradation of the stored energy was observed. The response to the H α /D α intensity near GP almost corresponds to the quantity of fuelling by GP, while the strong reduction in the H α /D α intensity far from GP was observed at $t=238$ ms in accordance with an increase in the edge AXUV intensity. After that, the stored energy reached a maximum value, which corresponds to the diamagnetic beta of 0.8%.

The radial profiles of the electron temperature (T_e), the electron density (n_e), the ion temperature (T_i) and the H α /D α intensity ($I_{H\alpha/D\alpha}$) are plotted in Figs. 2(a)-(b) before ($t=210$ ms), just after (232ms) and 20ms after (242ms) HIGP. The effect of the Shafranov shift due to the plasma beta is not considered yet. Due to HIGP, n_e at the core region increased twice from $t=210$ ms to 232ms, while the change in T_e was small. At $t=242$ ms, T_e and T_i in the peripheral region increased remarkable, then the increase in the stored energy was mainly due to the increase in the edge temperatures. At the timing of $t=242$ ms, the maximum density around $1 \times 10^{20} \text{ m}^{-3}$ was observed in the core region. The H α /D α intensity decreased about 50% from $t=232$ ms to 242ms, while its profile shape did not change significantly. Since the change in n_e was small between the two timings, this phenomenon indicates the reduction in the hydrogen density in the plasma after HIGP.

The power spectrum of the density fluctuation at the edge region ($r/a=0.9$) measured by beam emission spectroscopy [4] is shown in Fig. 3. At the time when the

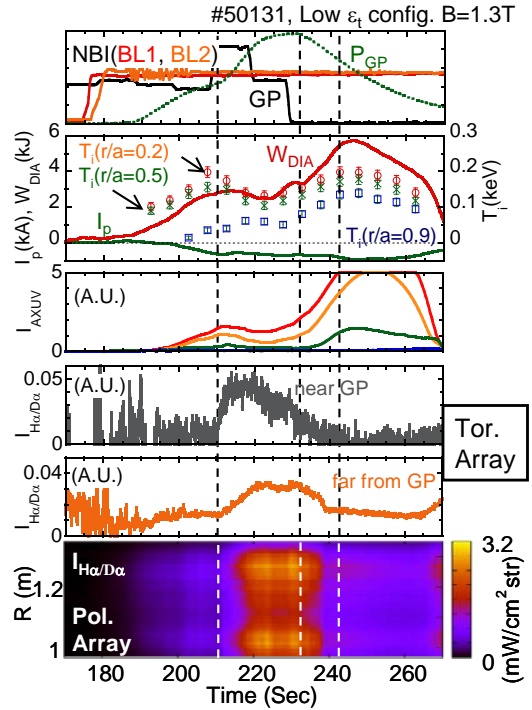


Fig. 1. Time evolution of heating/fueling, stored energy (W_{DIA}), toroidal current (I_p), ion temperature, AXUV intensity (I_{AXUV}) and H α /D α line emission intensity ($I_{H\alpha}$).

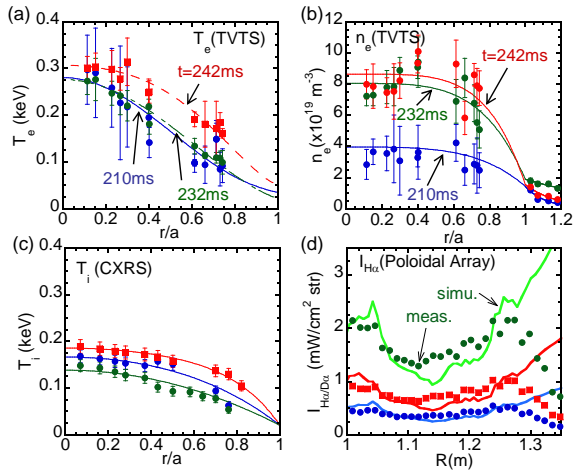


Fig. 2. Radial profile of (a) electron temperature, (b) electron density, (c) ion temperature and (d) H α /D α intensity before ($t=210$ ms), during (232ms) and after (242ms) intense GP. The lines for T_e , n_e and T_i are the fitting curves for them. The H α emission intensity calculated by simulation is plotted by the solid lines.

$\text{H}\alpha/\text{D}\alpha$ intensity started to decrease ($t=232\text{ms}$), the density fluctuation in the low frequency range ($f=0\text{-}25\text{kHz}$) became strong, while it disappeared at the same timing as the drop of the $\text{H}\alpha/\text{D}\alpha$ emission intensity ($t=238\text{ms}$). Similar tendency in the density fluctuation was observed in the whole plasma region.

The change in the parallel rotation velocity (v_{\parallel}) was also observed after the drop of the $\text{H}\alpha/\text{D}\alpha$ emission intensity. Figure 4 shows the radial profile of the parallel rotation velocity measured by the charge exchange recombination spectroscopy [5]. The v_{\parallel} shear became stronger in the edge region from $t=232\text{ms}$ to $t=247\text{ms}$.

3. Discussions

To reveal the behavior of the particle/energy confinement as well as the effect of the edge neutrals in the high density discharge by HIGP, we calculated the neutral particle transport using a Monte-Carlo simulation [6] and the beam momentum/power deposition profiles using a Fokker-Planck analysis [7].

For the neutral particle transport simulation, a full-torus plasma mesh was used, which was based on the geometry of the vacuum vessel and magnetic configuration. Three types of the particle source were introduced as the initial condition, the gas fueling from GP, the hydrogen recycling which was uniformly distributed at the wall surface and the recycling from "footprint". The source position of the footprint at the wall was determined from the collisionless orbit calculation. The amount of the uniformly distributed wall and footprint sources were determined so as to reproduce the measurement data. The solid lines in Fig. 2(d) show the emission intensity calculated by the simulation. The calculated intensity using the three particle sources is almost consistent with the measurement data. However, some discrepancy can be seen in the outer torus side ($R > 1.3\text{m}$). The improvement in the particle source distribution is required for more precise estimation. From the simulation, the edge neutral hydrogen density decreases by 50% after the intense GP. Therefore, the decrease in the charge exchange or radiation losses in the peripheral region may have a contribution to improve the plasma performance.

Figure 5(a) and (b) show the NB absorption power and external momentum profiles calculated by the Fokker-Planck analysis. The absorption power at the core region gradually decreased with time, because

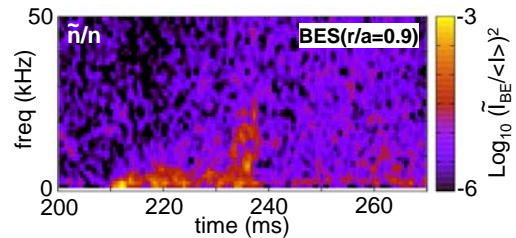


Fig. 3. Time evolution of the power spectrum measured by beam emission spectroscopy

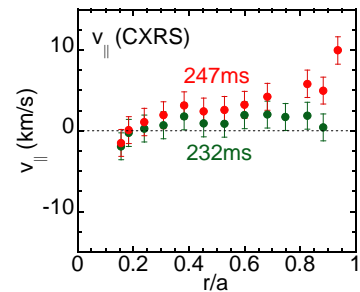


Fig. 4. Radial profile of the parallel rotation velocity measured by charge exchange recombination spectroscopy.

the absorption power for the counter NB decreases with increasing the density from $t=210\text{ms}$ to 242ms . The change in the power deposition profile from $t=232$ to 242ms is small, while the increase in T_i and T_e in the peripheral region, as shown in Fig. 2(a) and 2(c), was significant between the two timings. In addition, the change in the parallel rotation velocity between the two timings would not be explained by the small change in the momentum input. Now, we are applying the transport code into Heliotron J plasma and the energy and momentum transport will be discussed near future taking the neutral effect at the peripheral region into account.

The energy confinement time defined as $\tau_e = W_{\text{DIA}} / (\int p_{\text{NB}} dV - dW_{\text{DIA}}/dt)$, is plotted in Fig. 6 in conjunction with the comparison of the ISS95 scaling law. A remarkable improvement in the energy confinement was observed at $t=242\text{ms}$.

4. Summary

We have tried the high density plasma operation using the HIGP method. The electron density around $1 \times 10^{20} \text{ m}^{-3}$ was achieved by the combination of low α configuration and HIGP. The characteristics of the plasma profile under the high density condition is summarized as (1) the increase in the peripheral T_i and T_e with flat density profile (2) the reduction in the density fluctuation in accordance with the sudden drop of the H α /D α emission intensity and (3) the relatively high v_{\parallel} shear at the peripheral region. Although the transport analysis is required, the reduction in the neutral density in the peripheral region causes decrease in the charge exchange or radiation losses, which may have a contribution to improve the plasma performance.

References

- [1] T. Mizuuchi, F. Sano, et al., IAEA-FEC2012, 8-13 Oct (2012), San Diego, USA, EX/P3-07.
- [2] S. Kobayashi, K. Nagaoka, et al., 37th EPS conf, 21-25 Jun (2010), Dublin, Ireland, P1.1053.
- [3] S. Kobayashi, K. Nagasaki, et al., Nucl. Fusion **51** 062002 (2011).
- [4] S. Kobayashi, S. Kado, et al., Rev. Sci. Inst. **83** 10D535 (2012).
- [5] H. Lee, S. Kobayashi, et al., Plasma Phys Contr. Fusion **55** 035012 (2013).
- [6] S. Kobayashi, et al., Rev. Sci. Inst. **77**, 10E527 (2006)
- [7] S. Murakami, N. Nakajima, M. Okamoto, Trans. Fusion Tech. **27**, 256 (1995).

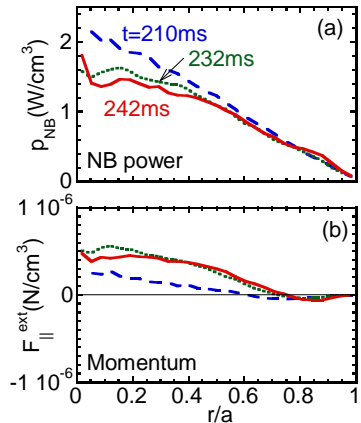


Fig. 5. Radial profile of (a) total NB absorption power and (b) momentum input at $t=210, 232$ and 242ms .

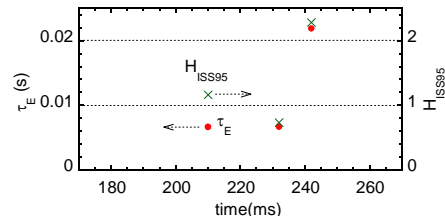


Fig. 6. Time history of the energy confinement time and the ratio to the ISS95 scaling law.